pubs.acs.org/acschemicalbiology

Article

Establishing a Cell-Free Glycoprotein Synthesis System for Enzymatic *N*-GlcNAcylation

Madison A. DeWinter,[¶] Derek A. Wong,[¶] Regina Fernandez, Weston Kightlinger, Ariel Helms Thames, Matthew P. DeLisa, and Michael C. Jewett*

Cite This: *ACS Chem. Biol.* 2024, 19, 1570−1582

Read Online

ACCESS | Metrics & More | Article Recommendations | Supporting Information

ABSTRACT: *N*-linked glycosylation plays a key role in the efficacy of many therapeutic proteins. One limitation to the bacterial glycoengineering of human *N*-linked glycans is the difficulty of installing a single *N*-acetylglucosamine (GlcNAc), the reducing end sugar of many human-type glycans, onto asparagine in a single step (*N*-GlcNAcylation). Here, we develop an *in vitro* method for *N*-GlcNAcylating proteins using the oligosaccharyltransferase PglB from *Campylobacter jejuni*. We use cell-free protein synthesis (CFPS) to test promiscuous PglB variants previously reported in the literature for the ability to produce *N*-GlcNAc and successfully determine that PglB with an N311V mutation ($PglB^{N311V}$) exhibits increased GlcNAc transferase activity relative to the wild-type enzyme. We then improve the transfer efficiency by producing CFPS extracts enriched with $PglB^{N311V}$ and further optimize the reaction conditions, achieving a 98.6 ± 0.5% glycosylation efficiency. We anticipate this method will expand the glycoengineering toolbox for therapeutic research and biomanufacturing.

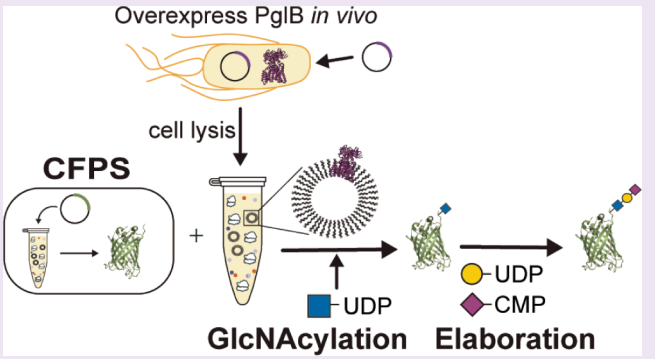

INTRODUCTION

N-linked glycosylation, the covalent attachment of glycans to asparagine residues on proteins, is an important post-translational modification that plays a key role in a therapeutic protein's pharmacokinetics,[1,2] stability,[3,4] function,[5−7] and immunogenicity.[8] In human *N*-linked glycans, the reducing end sugar, or the sugar directly attached to the protein, is *N*-acetylglucosamine (GlcNAc). This reducing end GlcNAc is one component of a conserved trimannosyl structure composed of two GlcNAc residues followed by three mannose residues, which may be further elaborated upon with additional sugars such as mannose, galactose, fucose, glucose, and sialic acid that create the full glycan structure. These sugar residues can be combined in numerous ways to create a wide array of different glycans that can be classified into high mannose, complex, and hybrid structures.[9] Even small changes to these structures can affect a therapeutic protein's function, as in the presence of terminal sialic acid residues,[10−13] or efficacy, as in the presence of fucose on antibody glycans.[14] Engineering the identity of these structures, studying their therapeutic effects, and establishing robust methods for producing glycoproteins with homogeneous, human-type glycans is a major focus in the field of glycobiology.[15]

Despite the importance of a protein's glycosylation profile on its stability and function, current methods for producing glycoproteins often yield heterogeneous glycan profiles. For example, *in vivo* protein expression in Chinese hamster ovary (CHO) cells produces protein products with heterogeneous complex bi-, tri-, and tetra-antennary structures, which makes it difficult to understand the specific biological response to a particular therapeutic glycoform and creates challenges with developing robust and reproducible biomanufacturing processes.[16,17] Recent advances in the field have worked to address this issue through various glycoengineering strategies,[18] including establishing a genetically modified CHO strain capable of producing glycoproteins with only a single *N*-linked GlcNAc residue, a Gal-GlcNAc disaccharide, or an α-2,3-sialylated trisaccharide, reducing the overall product glycan heterogeneity[19] and providing a handle for additional chemoenzymatic elaboration.[20] While proteins produced using this cell line displayed favorable pharmacokinetic properties, the reliance on genetically modified mammalian cell lines complicates adaptation of the workflow to other glycoforms without genomic changes.

Received: April 2, 2024
Revised: May 30, 2024
Accepted: June 3, 2024
Published: June 27, 2024

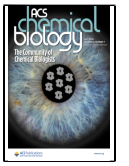

https://doi.org/10.1021/acschembio.4c00228
ACS Chem. Biol. 2024, 19, 1570−1582

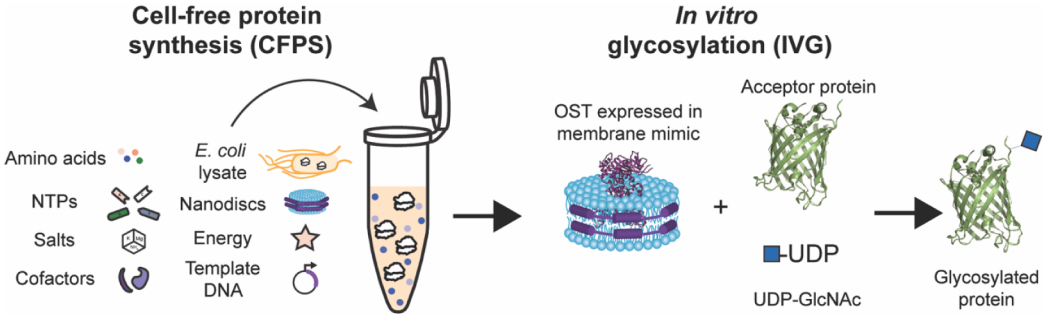

Figure 1. Cell-free protein synthesis (CFPS) and *in vitro* glycosylation (IVG) can be combined to synthesize glycoproteins *in vitro*. CFPS utilizes the native transcription and translation machinery in cell extracts to synthesize proteins by supplying a template DNA, additional cofactors, and an energy source. Nanodiscs provide a membrane mimic and enable the soluble expression of active membrane-bound proteins. After expression in CFPS, OSTs can be combined with appropriate sugar donors, necessary cofactors, and an acceptor protein to produce glycoproteins *in vitro*.

In comparison to *in vivo*–based approaches, the modularity and open reaction environment of cell-free or *in vitro* glycosylation (IVG) systems could aid in the development of new glycoprotein production methods. Indeed, recent work in the field has sought to create routes to glycosylated proteins and peptides using glycosyltransferases heterologously expressed in living *Escherichia coli*[21−28] or in cell-free protein synthesis (CFPS)[29−33] and subsequently assembled in IVG reactions. To date, there have been several attempts to use these systems to create glycoproteins harboring a single *N*-GlcNAc residue, which differentiate from the strategy presented in this work through the use of (i) multienzyme methods with sugar donors that are not commercially available,[21] (ii) synthetic GlcNAc donor substrates composed of GlcNAc coupled to chemically synthesized polyisoprenol sugar pyrophosphates,[34,35] (iii) cell-based biosynthesis of larger bacterial or eukaryotic *N*-linked glycan structures that must be subsequently trimmed *in vitro* by a glycosidase,[6,36] or (iv) complicated multistep chemical synthesis routes[37−40] to produce the priming GlcNAc residue. Once formed, this residue can be elaborated to generate the final desired glycoform.

CFPS systems[41] using extracts derived from *E. coli* have emerged as an attractive tool for both producing glycoproteins and for prototyping glycosylation parts and systems.[29] In CFPS, extracts are combined with various cofactors, energy substrates, and DNA encoding the protein of interest to perform *in vitro* transcription and translation reactions to synthesize desired proteins.[41] Due to the inherent lack of protein glycosylation machinery in *E. coli*, these lysates offer a blank slate for constructing glycosylation pathways. To date, cell-free systems have been used to produce conjugate vaccines[42−44] and sialoglycoproteins[45] as well as understand glycosyltransferase acceptor sequence preference[46] and prototype protein glycosylation pathways.[47] To the best of our knowledge, however, an integrated system for the *in vitro* synthesis of both the acceptor protein and an undecaprenyl phosphate–linked GlcNAc followed by the subsequent enzymatic glycosylation of the acceptor protein with a single GlcNAc residue has not been reported.

In this study, we set out to expand the range of glycans accessible to CFPS by developing a modular approach to produce glycoproteins with human-like glycans originating with an *N*-linked GlcNAc as the reducing end sugar. Building off previous efforts that have shown PglB mutations with enhanced substrate specificity[48] and *N*-GlcNAcylation with chemically synthesized lipid linked substrates,[34,35] we use CFPS to determine that a promiscuous variant of the oligosaccharyltransferase (OST) PglB from the organism *Campylobacter jejuni* exhibits enhanced *in vitro* N-GlcNAcylation capabilities compared to wild type. Next, we optimize the IVG reaction conditions to achieve > 98% GlcNAcylation efficiency. We then demonstrate that our system depends on the activity of endogenous WecA to produce an intermediary GlcNAc linked to a carrier lipid undecaprenyl phosphate. Finally, we show the sequential elaboration of the priming GlcNAc residue with a galactose and an α-2,6-sialic acid to form a sialylated trisaccharide.

RESULTS

The goal of this work was to create a one-step, *in vitro* method for producing proteins with a priming *N*-GlcNAc. To this end, we explored if the *Campylobacter jejuni* OST PglB could efficiently transfer a single GlcNAc residue in a cell-free reaction supplemented with commercially available uridine diphosphate *N*-acetylglucosamine (UDP-GlcNAc) without requiring the addition of chemically synthesized lipid-linked GlcNAc. PglB has attracted considerable attention for its ability to transfer *en bloc* many glycan polymers, such as O-antigens used to produce conjugate vaccines,[42−44,48−53] to proteins. Beyond O-antigens, PglB has also shown the ability to transfer smaller glycans that could be used for the bottom-up construction of complex glycans on proteins, including monosaccharides such as bacillosamine,[54] 2,4-diacetamido-2,4,6-trideoxyhexose (DATDH),[55] and GlcNAc.[34,35] PglB can also be mutated to increase glycan substrate promiscuity.[48,56]

PglB^{N311V} Can *N*-GlcNAcylate Proteins in a One-Step, *In Vitro* Glycosylation Reaction. We tested the wild-type PglB sequence as well as promiscuous mutants containing the single mutation N311V (PglB^{N311V}) or set of mutations S80R-Q287P-N311V (PglB$^{S80R\text{-}Q287P\text{-}N311V}$).[48] To facilitate rapid prototyping, we first expressed PglB variants in nanodisc-supplemented CFPS reactions. Because PglB is a membrane-bound protein, nanodiscs are important supplements for the reaction that serve as membrane mimics to facilitate proper folding. IVG reactions were then performed by mixing the expressed OST variant with a superfolder green fluorescent protein (sfGFP) acceptor protein containing a C-terminal DQNAT sequon (a short stretch of amino acids recognized by the OST)[57,58] and StrepII-tag (to facilitate purification), as well as UDP-GlcNAc and manganese chloride, which serves as a cofactor for PglB (Figure 1). After overnight incubation at 30 °C, the sfGFP acceptor protein was purified, digested with

https://doi.org/10.1021/acschembio.4c00228
ACS Chem. Biol. 2024, 19, 1570−1582

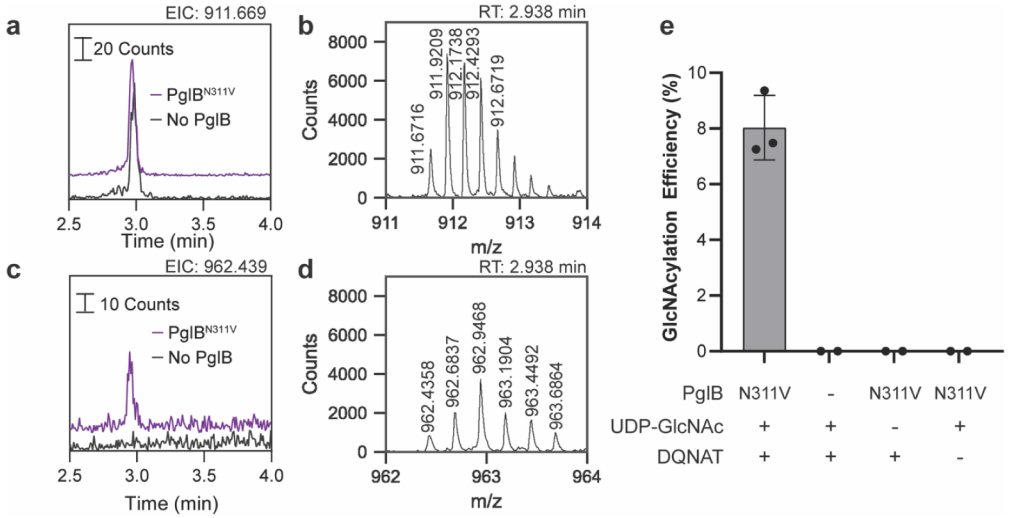

Figure 2. PglB^{N311V} expressed in nanodisc-supplemented CFPS can modify an acceptor protein with *N*-GlcNAc in an IVG reaction. (a) The extracted ion chromatograms (EICs) for reactions containing PglB^{N311V} (purple) and no PglB (black) contain a peak at 2.9 min corresponding to the + 4 charge state of the mass to charge ratio of the aglycosylated tryptic peptide. (b) The isotope distribution for the PglB^{N311V} sample at 2.9 min is shown. The observed monoisotopic mass (3642.6544) corresponds to the theoretical monoisotopic mass (3642.6458 Da) of the aglycosylated peptide with an error of 2.4 ppm. (c) EICs for the + 4 charge state of the mass to charge ratio of the GlcNAcylated tryptic peptide in reactions containing PglB^{N311V} (purple) and without PglB (black) are shown. There is only a peak at 2.9 min in the reaction with PglB^{N311V}. (d) The isotope distribution for the PglB^{N311V} sample confirms the presence of the GlcNAcylated peptide. The observed monoisotopic mass (3845.7112) corresponds to the theoretical monoisotopic mass (3845.7252 Da) with an error of 3.6 ppm. Mass spectrometry data are representative of at least 2 independent reaction replicates. (e) Quantification of GlcNAcylation efficiency of IVG reactions using PglB^{N311V} expressed in nanodisc-supplemented CFPS is shown. Three (n = 3) replicates were performed for the N311V + UDP-GlcNAc + DQNAT sample, and two (n = 2) replicates were performed for the other samples, with each replicate composed of an individual IVG reaction. Error bars represent the average error.

trypsin, and desalted with C18 peptide clean up columns for analysis by tandem reverse phase liquid chromatography−mass spectrometry (LC-MS) to look for evidence of transfer of the GlcNAc onto asparagine. Reactions utilizing either PglB^{N311V} (Figure 2) or PglB$^{S80R-Q287P-N311V}$ (Supplementary Figure 1) yielded GlcNAcylated tryptic peptides, while no transfer was observed in reactions utilizing the wild-type OST (Supplementary Figure 2).

Because there was a more distinct and abundant isotope distribution for reactions containing PglB^{N311V}, we set out to further characterize this reaction to validate the GlcNAc transfer. We performed IVG reactions containing PglB^{N311V} expressed in nanodisc CFPS and compared them to negative control reactions without PglB. In the extracted ion chromatograms (EICs) using the mass to charge ratio corresponding to the aglycosylated peptide fragment (Figure 2a), a peak is observed at approximately 2.97 min in the elution for both samples. In the spectrum of this peak for the PglB^{N311V} sample, a clear isotope distribution is observed (Figure 2b) for a + 4 charged species, where the observed mass matches the theoretical mass of the aglycosylated tryptic peptide. In contrast, we only observed a peak at approximately 2.95 min in the EIC for the mass to charge ratio of the GlcNAcylated tryptic peptide when PglB^{N311V} was added to the reaction mixture (Figure 2c). Additionally, the isotope distribution in the PglB^{N311V} sample (Figure 2d) shows a spectrum where the observed mass matches the theoretical mass of the GlcNAcylated peptide. Further evidence of the presence of both the aglycosylated and GlcNAcylated peptides is given in the collision induced dissociation (CID) MS/MS fragmentation spectra for both ions, where the sequence of the tryptic peptide was confirmed (Supplementary Figure 3).

Quantification of the abundance of GlcNAcylation was performed using the area under the curves of the EICs for both the aglycosylated and GlcNAcylated species. When the OST mutant, the activated sugar donor (UDP-GlcNAc), and the correct acceptor sequon (DQNAT) were present, the transfer efficiency was 8.0 ± 1.2% (Figure 2e). However, if PglB, UDP-GlcNAc, or the DQNAT sequon was absent, then there was no observed transfer of the GlcNAc residue. In the no DQNAT acceptor samples, an AQNAT sequon was used because it is known that PglB requires a sequon with an acidic residue at the −2 position.[57] Representative EICs and isotope distributions for the reactions containing no PglB (Supplementary Figure 4), no UDP-GlcNAc (Supplementary Figure 5), or using an acceptor protein with the AQNAT sequon (Supplementary Figure 6) are provided in the Supporting Information.

***N*-GlcNAcylation Efficiency Can Be Improved Using Extracts Enriched with PglB and Optimizing Glycosylation Reaction Conditions.** We next sought to improve the GlcNAcylation efficiency in our system and explore a more cost-effective method for PglB synthesis to use in IVG reactions. Therefore, we assessed whether we could improve the yields of *N*-GlcNAcylated protein in our IVG reactions with extracts enriched with PglB expressed *in vivo* (rather than PglB expressed in nanodisc supplemented CFPS reactions) and by optimizing other components of the IVG reaction. To produce the enriched extracts, we transformed a plasmid encoding PglB into CLM24 cells and induced expression during cell growth. After harvesting, we processed the extracts in a manner previously demonstrated to increase the number of membrane vesicles retained within the lysate.[33] These lysates were then mixed with a separate CFPS reaction used to express the acceptor protein along with activated UDP-

https://doi.org/10.1021/acschembio.4c00228
ACS Chem. Biol. 2024, 19, 1570−1582

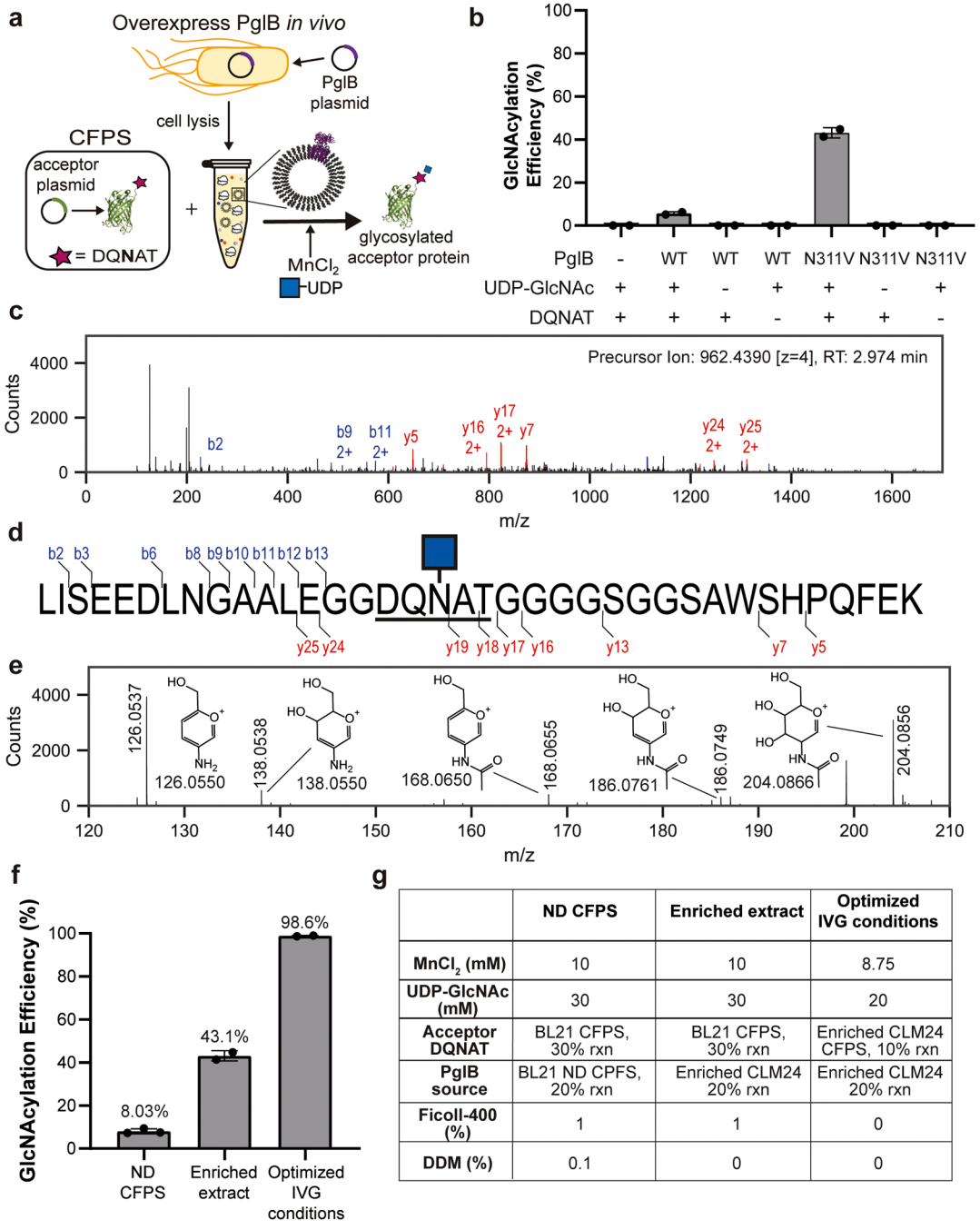

g

	ND CFPS	Enriched extract	Optimized IVG conditions
$MnCl_2$ (mM)	10	10	8.75
UDP-GlcNAc (mM)	30	30	20
Acceptor DQNAT	BL21 CFPS, 30% rxn	BL21 CFPS, 30% rxn	Enriched CLM24 CFPS, 10% rxn
PglB source	BL21 ND CPFS, 20% rxn	Enriched CLM24 20% rxn	Enriched CLM24 20% rxn
Ficoll-400 (%)	1	1	0
DDM (%)	0.1	0	0

Figure 3. Using extracts enriched with PglB and modulating additional IVG conditions increases overall *N*-GlcNAcylation efficiency. (a) Enriched extracts are prepared by overexpressing PglB during cell growth prior to cell lysis. PglB-enriched lysate can then be mixed with a CFPS reaction separately expressing the carrier protein along with UDP-GlcNAc and $MnCl_2$ to perform the IVG reaction. (b) Quantification of GlcNAcylation efficiency for each of the conditions tested using extracts enriched with PglB is shown. Two replicates were performed for each sample ($n = 2$), with each replicate composed of a separate IVG reaction, and error bars represent the average error. (c) The MS/MS fragmentation spectrum for the GlcNAcylated tryptic peptide from IVG reactions using extracts enriched with PglB is shown. Prominent b and y ions are labeled in blue and red, respectively, on the spectrum. (d) All identified ions in the spectrum shown in (c) are labeled on the tryptic peptide sequence. (e) In the 120−210 m/z range in the spectrum shown in (c), characteristic oxonium ions expected from the fragmentation of GlcNAc are observed and labeled appropriately. (f) Quantification of GlcNAcylation efficiency for IVG reactions using $PglB^{N311V}$ is shown following each round of reaction condition optimization. (g) Conditions for each GlcNAcylation reaction in panel f are summarized in the table. Three ($n = 3$) replicates were performed for the ND CFPS sample and two ($n = 2$) replicates were performed for the other samples, with each replicate composed of a separate IVG reaction. Error bars represent the average error. The nanodisc CFPS data are repeated from Figure 2e, and the enriched extract data are repeated from Figure 3b.

GlcNAc sugar donors and manganese chloride as a cofactor, to perform the *in vitro* glycosylation reactions (Figure 3a).

Using the enriched extract approach improved the *N*-GlcNAcylation efficiency 5-fold to 43.1 ± 2.4% when using $PglB^{N311V}$ and permitted detection of 5.6 ± 0.7% *N*-

https://doi.org/10.1021/acschembio.4c00228
ACS Chem. Biol. 2024, 19, 1570−1582

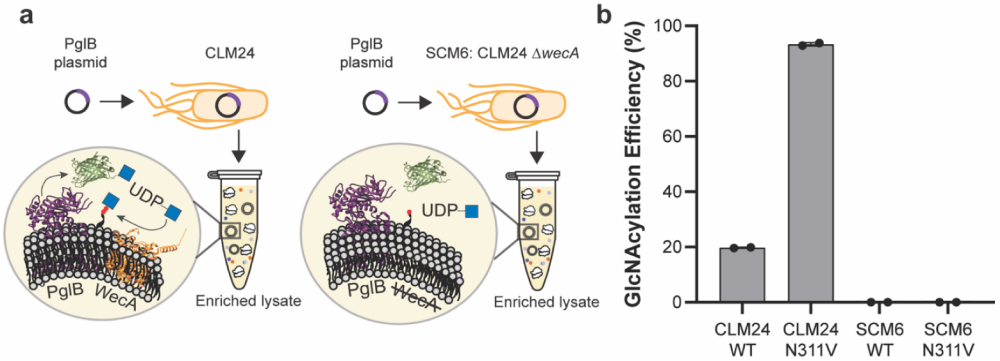

Figure 4. PglB likely transfers the single GlcNAc onto the acceptor protein *via* a lipid-linked intermediate. (a) The CLM24 strain has endogenously expressed WecA, which is an enzyme that transfers UDP-GlcNAc to undecaprenyl phosphate to synthesize undecaprenyl-pyrophosphoryl-GlcNAc, while SCM6 lacks WecA (CLM24 Δ*wecA*). (b) Quantification of the GlcNAcylation efficiency for reactions utilizing each of the tested enriched extracts. Two replicates were performed for each sample ($n = 2$), with each replicate composed of a separate IVG reaction, and error bars represent the average error.

GlcNAcylation by wild-type PglB (Figure 3b). No GlcNAcylation was observed in negative control reactions that either lacked PglB, or UDP-GlcNAc, or used the nonfunctional AQNAT sequon instead of a DQNAT sequon (Figure 3b). Extracted ion chromatograms and isotope distributions are available for each of the conditions in Figure 3b (Supplementary Figures 7−13). Collision-induced dissociation (CID) MS/MS of the GlcNAcylated tryptic peptide confirms the sequence of the GlcNAcylated peptide (Figure 3c,d). The y24 and y25 ions incorporate the asparagine residue that is GlcNAcylated in the DQNAT sequon, while the smaller y ions confirm that the modification does not occur downstream of the asparagine in the sequon. Specifically, the presence of the y17 and y18 ions explicitly show that the GlcNAcylation is not an *O*-GlcNAc on the threonine residue in the DQNAT sequon. Together, the data suggest that the GlcNAc modification is on the asparagine residue within the DQNAT sequon, as expected. The CID MS/MS spectrum that confirms the sequence of the aglycosylated peptide in the same sample is given in Supplementary Figure 14. Additionally, when the focus is on the 120−210 m/z range of the spectrum presented in Figure 3c, many characteristic oxonium ions are observed (Figure 3e). These oxonium ions are fragments from the GlcNAc sugar residue itself and are commonly seen in CID MS/MS spectra from *O*-GlcNAc modifications,[59,60] providing further evidence that the GlcNAcylation modification is occurring as expected.

After improving the GlcNAcylation efficiency by using extracts enriched with *in vivo*−expressed PglB, we sought to further increase the transfer efficiency by optimizing additional IVG reaction components. We hypothesized that multiple parameters could affect *N*-GlcNAcylation efficiency, including the concentration of manganese chloride, UDP-GlcNAc, acceptor protein, PglB-enriched extract, Ficoll-400, and N-dodecyl-beta-maltoside (DDM) in the final IVG reactions. To explore which parameters had the greatest impact on glycosylation efficiency, we carried out a definitive screening design experiment,[61] incorporating each of these identified variables. Due to the reaction's dependence on PglB, we assumed that adding additional PglB to the reaction would not negatively impact GlcNAcylation efficiency and expressed the acceptor protein in extracts enriched with PglB. To our surprise, GlcNAcylation efficiency was dramatically improved by optimizing multiple factors (Supplementary Figure 15). The most important variables were maximizing the amount of UDP-GlcNAc and the enriched extract supplemented to the reaction. Specifically, we could achieve 98.6 ± 0.5% GlcNAcylation with a final concentration of 8.75 mM manganese chloride, 25 mM UDP-GlcNAc, 10% (v/v) of acceptor protein produced in CFPS using the enriched extract, 20% (v/v) of additional extract enriched with $PglB^{N311V}$, 0% Ficoll-400, and 0% DDM (Figure 3f,g). Using optimized conditions, the GlcNAcylation efficiency for IVG reactions using extract enriched with wild-type PglB was 39.5 ± 4.5% (Supplementary Figure 16), confirming the superiority of $PglB^{N311V}$ for performing the GlcNAcylation in this setting.

GlcNAc Transfer by PglB Likely Occurs *via* a Lipid-Linked Intermediate. Given that PglB typically glycosylates proteins with glycans that are linked to the lipid carrier undecaprenyl phosphate,[54,62−64] we were interested in determining whether a similar lipid-linked GlcNAc intermediate was being produced in our reactions. Importantly, we note that CLM24, the *E. coli* strain used to make our PglB-enriched extracts, natively expresses WecA, a polyprenyl-phosphate N-acetylhexosamine-1-phosphate transferase that catalyzes the transfer of GlcNAc-1-phosphate from UDP-GlcNAc to a carrier undecaprenyl phosphate lipid.[65] Supplementation of our reactions with UDP-GlcNAc could therefore enable the production of undecaprenyl phosphate-linked GlcNAc that PglB can use as a substrate for subsequent GlcNAcylation reactions.

To test this WecA-centered hypothesis, enriched extracts were produced for both wild-type and $PglB^{N311V}$ overexpressed in a standard CLM24 source strain and an SCM6 source strain (CLM24 Δ*wecA*) (Figure 4a). Although GlcNAcylation was observed when CLM24 extracts were enriched in either wild-type or $PglB^{N311V}$ and IVG reactions were assembled under optimized conditions from Figure 3, there was no GlcNAcylation observed when SCM6 extracts were enriched in either wild-type or $PglB^{N311V}$. This suggests that the GlcNAcylation reaction proceeds through a lipid-linked intermediate *via* a WecA-dependent mechanism (Figure 4b).

To confirm PglB overexpression in each of the four enriched extracts tested, we performed a Western blot against the C-terminal FLAG-tag encoded in PglB (Supplementary Figure 17a). While we confirmed the presence of PglB in all four extracts, densitometry analysis revealed that the concentration of PglB is approximately 5−10 × higher in the CLM24 extracts

https://doi.org/10.1021/acschembio.4c00228
ACS Chem. Biol. 2024, 19, 1570−1582

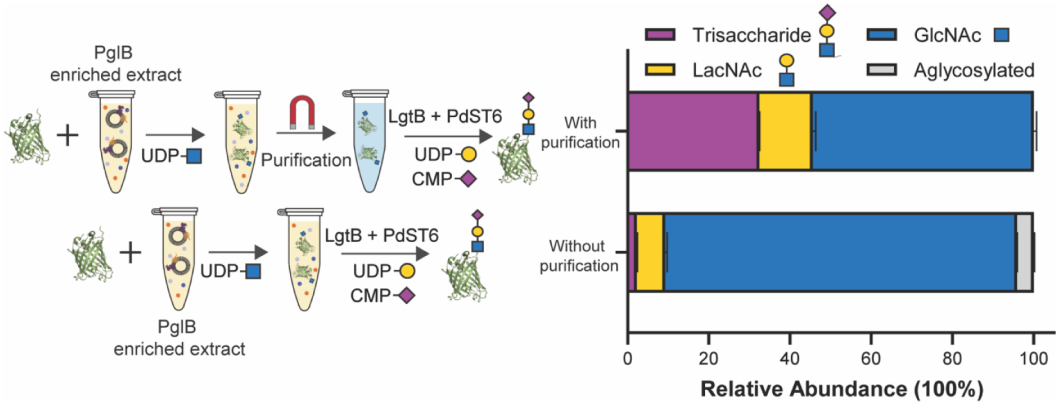

Figure 5. The GlcNAcylated protein can be elaborated with galactose and sialic acid to create a trisaccharide sialyl *N*-acetyllactosamine glycoform. LgtB and PdST6 were used to add galactose to the GlcNAc and sialic acid to the galactose residues, respectively. The results from the two glycosylation schemes are shown. In the "without purification" samples, the GlcNAcylation reaction is first performed overnight with PglB. Then, the two elaborating glycosyltransferases, LgtB and PdST6, are added to the same *in vitro* glycosylation reaction with the nucleotide-activated donor sugars and incubated overnight for a second night. In the "with purification" workflow, the GlcNAcylation reaction with PglB is performed in an overnight incubation first. The GlcNAcylated acceptor protein is then purified, and a second IVG reaction is performed to add galactose and sialic acid by using LgtB and PdST6. Two independent replicates were performed for each sample (n = 2), with each replicate composed of a separate IVG reaction, and error bars represent the average error.

when compared to the SCM6 extracts. Therefore, to ensure that the lack of GlcNAcylation observed in reactions using SCM6-derived extract is not a result of a lower concentration of PglB, a volume correction experiment was also performed. As shown in Supplementary Figure 17b, even when normalizing for equivalent PglB concentrations by adjusting the volume of enriched extract added to the IVG reactions, we do not observe GlcNAcylation in reactions utilizing SCM6-derived enriched extracts. These results suggest that WecA is essential to the GlcNAcylation reaction and that glycosylation likely occurs *via* a lipid-linked intermediate. Extracted ion chromatograms and isotope distributions for the 4 samples in Figure 4b are provided in Supplementary Figures 19 and 20.

Elaboration of the Priming GlcNAc to Produce a Trisaccharide Siayl-LacNAc Structure. To demonstrate the utility of our one-step, *in vitro* GlcNAcylation workflow in the bottom-up engineering of glycoproteins, we performed reactions to elaborate on the GlcNAc priming sugar to produce a biologically relevant human-like glycan. Previous work has demonstrated that decorating proteins and peptides with a trisaccharide structure composed of either Neu5Ac-α-2,6-Galβ-1,4-GlcNAc[2,66] or Neu5Ac-α-2,3-Galβ-1,4-GlcNAc[19] can improve the molecules' pharmacokinetic stability. We therefore sought to produce one of these trisaccharides using a completely *in vitro* enzymatic approach. LgtB, a glycosyltransferase from *Neisseria meningitidis*, has been shown to install galactose onto GlcNAc in a β-1,4 linkage, and PdST6, a glycosyltransferase from *Photobacterium damselae*, has been shown to install sialic acid in an α-2,6 linkage.[22,45,47] We incorporated these enzymes and the appropriate nucleotide-activated sugar donors, uridine diphosphate α-D-galactose (UDP- galactose) and cytidine monophosphate sialic acid (CMP-sialic acid), into our reaction solution to perform elaboration to a sialylated *N*-acetyllactosamine (sialyl-LacNAc) structure.

A definitive screening design experiment was used to explore the effect of LgtB, PdST6, UDP-galactose, and CMP-sialic acid concentrations on the extent of protein-linked trisaccharides produced in our reactions. Additionally, a one-day scheme, in which all three enzymes and donor sugars were combined at once in the IVG reaction, was compared to a two-day scheme in which the GlcNAcylation reaction was performed separately from the elaboration reaction. The definitive screening design experiment revealed that the two-day scheme was important for trisaccharide elaboration as we did not observe the production of proteins with the trisaccharide in any of the samples run using the one-day scheme. Generally, higher concentrations of glycosyltransferase enzymes and nucleotide-activated sugar donors also increased the yield of the trisaccharide glycoform (Supplementary Figure 21). However, the highest trisaccharide conversion observed in this experiment was only 2.2 ± 0.2%.

We hypothesized that the low yield of the sialyl-LacNAc glycoform may be due to LgtB and PdST6 elaborating on excess lipid-linked GlcNAc present in the IVG reaction rather than on proteins previously GlcNAcylated by PglB or that reaction conditions optimal for GlcNAcylation by PglB are not optimal for LgtB and/or PdST6 activity. To this end, we modified our two-day glycosylation scheme by incorporating an affinity purification step after GlcNAcylation by PglB and before elaboration by LgtB and PdST6. Incorporating the affinity purification step into our workflow improved conversion efficiency to the sialyl-LacNAc glycoform 14-fold to 32.4 ± 0.1% (Figure 5). Extracted ion chromatograms and isotope distributions for the two samples presented in Figure 5 are provided in Supplementary Figures 22 and 23. While further optimization would need to be performed to achieve higher trisaccharide efficiency, such as those near 100% previously reported by Kightlinger et al.[47] and Tytgat et al.[67] for trisaccharides with a reducing end glucose, this level of efficiency is on par with that observed by Meuris et al.[19] for a glycan with a reducing end GlcNAc.

DISCUSSION

In this work, we describe a cell-free platform to enzymatically transfer a single GlcNAc residue to asparagine residues in a protein using a mutated PglB variant from *C. jejuni*. Through systematic optimization of both reaction conditions and production method for PglB, we demonstrate > 98% conversion of aglycosylated to glycosylated protein as well as

https://doi.org/10.1021/acschembio.4c00228
ACS Chem. Biol. 2024, 19, 1570−1582

elaboration of the GlcNAc priming sugar to a therapeutically relevant sialyl-LacNAc trisaccharide at efficiencies similar to those previously reported with more complicated, mammalian *in vivo*–based production methods.[19]

Key to our workflow is the use of crude *E. coli* cell lysates, which in addition to containing the transcription and translation machinery required for *in vitro* protein synthesis can also be enriched for enzymes required for glycosylation. Like other cell-free glycosylation methods, our system benefits from being an open reaction environment, enabling the facile manipulation of various reaction conditions to optimize for the production of predetermined glycoforms without relying on cell viability constraints. In contrast to *in vitro* systems using purified glycosyltransferases, our crude extracts retain membrane vesicles with membrane-associated proteins that are important for some glycosylation processes. We show that maintaining WecA, a membrane-associated enzyme, in our reactions is a key step in enabling the production of a lipid-linked GlcNAc intermediate and subsequent transfer of a single GlcNAc residue by PglB. Thus, our workflow effectively bridges the gap between modular, *in vitro*–based approaches and more complex *in vivo*–based approaches by taking advantage of membrane-based biological processes in an open *in vitro* reaction environment.

Through the incorporation of LgtB and PdST6 into our reaction scheme, we were able to produce a sialyl-LacNAc moiety that could improve the therapeutic properties of proteins and peptides by reducing protease degradation or immune cell recognition and clearance. Compared to other *E. coli*–based glycoengineering efforts for bottom-up construction of glycoproteins, we note that our sialyl-LacNAc glycosylation efficiency is lower than the efficiency at which other reported *in vivo*[67] or *in vitro*[47] approaches have installed a similar *N*-linked sialyllactose trisaccharide structure. Similar to our approach, these methods are completely enzymatic in which short sequons recognized by the appropriate glycosyltransferase are introduced to the C-terminus of the protein or in known flexible regions of the protein; this acceptor protein is then used in conjunction with three separate glycosyltransferases either through coexpression *in vivo* in the cytoplasm[67] or individual expression in CFPS and assembled into IVG reactions,[47] similar to the workflow described here. However, where our platform differs from these methods is the production of a GlcNAc reducing end sugar through PglB, rather than glucose through the asparagine (N)-glucosyltransferase (ApNGT) from the organism *Actinobacillus pleuropneumoniae*. Our installation of a GlcNAc reducing end sugar, which accurately mimics the reducing end sugar for glycoproteins produced in mammalian systems (including in humans), may be important for therapeutic function.

We anticipate that our workflow could also be combined with other advances in IVG methods to produce proteins with longer glycan polymers such as those commonly found with antibody therapeutics. For example, our one-step GlcNAcylation method could simplify chemoenzymatic transglycosylation approaches that utilize a mutated endoglycosidase (ENGase) to transfer chemically synthesized glycan polymers onto proteins with a single GlcNAc residue,[68,69] by removing the requirement of time-intensive mammalian cell culture and glycan trimming steps to produce the single GlcNAc residue. Our method could also be interfaced with other recent work developing *in vitro*, bead-based enzyme immobilization strategies for building glycosylation pathways.[22]

Future work will focus on expanding the capabilities of our platform for producing therapeutically relevant glycoproteins. For example, our proof-of-concept work presented here demonstrates efficient glycosylation of a model sfGFP construct using a C-terminal sequon. In some cases, *N*-GlcNAcylation at a specific internal residue within a protein may be desired (e.g., Asn297 in IgG). Due to the two-stage process described here by which a protein is first expressed and subsequently glycosylated in a second reaction, some internal residues within a fully folded protein may not be accessible for glycosylation by PglB. If desired glycosylation sites are poorly glycosylated using our system, future work could seek to further optimize the glycosylation reaction conditions to enable cotranslational glycosylation of amino acid residues that are inaccessible once the protein is fully folded. Additionally, overexpression of PglB often leads to slow cell growth rates due to the increased metabolic burden associated with expressing a membrane protein, which, in turn, can limit the protein yields obtained from the resulting cell extract. Scaling production of low-yielding, complex glycoproteins may therefore require optimization of PglB overexpression conditions to balance sufficient PglB concentration within the extract with the protein synthesis capabilities of the extract.

Looking ahead, our workflow provides a key step forward in efforts to produce human glycosylation patterns in synthetic systems. It holds promise to simplify the production process for proteins with defined human-like glycans, both natural and non-natural, and enable in-depth studies to understand and engineer the impact of glycan position and identity on a protein's bioactivity.

SIGNIFICANCE

An important feature of human *N*-linked glycans is an *N*-acetylglucosamine (*N*-GlcNAc) residue at the reducing end of the sugar, which is directly attached to asparagine residues in proteins. It has been difficult to install this priming sugar at high efficiencies with bacterial glycoengineering approaches. To address this limitation, we developed and optimized a simple, one-step, *in vitro* platform that integrates cell-free protein synthesis and an enzymatic process to *N*-GlcNAcylate proteins using a mutated version of a well-studied bacterial oligosaccharyltransferase, PglB, from *Campylobacter jejuni*. We demonstrate that cell-free extracts enriched in $PglB^{N311V}$ can be used for both cell-free protein synthesis of the acceptor protein and as the source of PglB in *in vitro* glycosylation reactions to enable > 98% conversion from aglycosylated to GlcNAcylated protein. In addition, we demonstrate that the GlcNAc priming sugar can be further elaborated to more complex, therapeutically relevant glycan structures. We anticipate that our cell-free system will aid in the development of biomanufacturing platforms for therapeutic proteins, as well as enable mechanistic studies to understand the effects of different glycoforms on biological responses.

METHODS

Material Availability. Plasmids and strains used in this study are available commercially or to interested parties via Addgene. Further information and requests for resources and reagents should be directed to and will be fulfilled by Michael C. Jewett (mjewett@stanford.edu).

https://doi.org/10.1021/acschembio.4c00228
ACS Chem. Biol. 2024, 19, 1570−1582

***E. coli* Strains.** BL21 Star (DE3): grown in Luria-Bertoni media at 37 °C for overnight culture and 2xYTPG media at 37 °C for extract preparation.

DH5α: grown in Luria-Bertoni media for DNA preparation or S.O.C. (Super Optimal broth with Catabolite repression) during recovery after transformation at 37 °C.

CLM24 Δ*lpxM*: grown in Luria-Bertoni media at 37 °C for overnight culture and either 2xYTPG or 2xYTP media at 37 °C for extract preparation along with the appropriate plasmid selection antibiotic (followed by 30 °C after induction for protein overexpression).

SCM6: grown in Luria-Bertoni media at 37 °C for overnight culture and 2xYTP media at 37 °C for extract preparation along with the appropriate plasmid selection antibiotic (followed by 30 °C after induction for protein overexpression).

759.T7.Opt: grown in Luria-Bertoni media at 34 °C for overnight culture and 2xYTPG media at 34 °C for extract preparation.

Plasmids. Plasmid DNA was prepared using a ZymoPURE Midi Kit or Qiagen HiSpeed Midiprep Kits according to manufacturer instructions. During the enriched extract preparation, kanamycin (50 μg/ml) was used to maintain the plasmid encoding PglB. A list of plasmids is provided in Table 1.

Table 1. A list of the Plasmids Used in this Study

plasmid	source
pSF-CjPglB^{N311V}-LpxE-KanR	this paper
pJL1-sfGFP-DQNAT-StrepII-6xHis	this paper
pJL1-sfGFP-AQNAT-StrepII-6xHis	this paper
pJL1 -CjPglB	this paper
pJL1- CjPglB^{N311V}	this paper
pJL1- CjPglB$^{S80R-Q287P-N311V}$	this paper
pJL1-LgtB	Kightlinger et al.[47]
pJL1-PdST6	Kightlinger et al.[47]

Cell Extract Preparation. For preparing extracts from BL21 Star™ (DE3) cells (Thermo Fisher C601003), cultures were grown at the 1 L scale in 2.5 L tunair shake flasks or at the 10 L scale in a Sartorius Stedim BIOSTAT Cplus bioreactor. Methods are similar to previous reports.[30,33,70] To start with, 2xYTPG was inoculated at an optical density at 600 nm (OD_{600}) = 0.06−0.08 and incubated at 37 °C with agitation at 250 RPM. At OD_{600} = 0.6, cells were induced for T7 RNA polymerase expression by adding IPTG to a final concentration of 0.5 mM. At OD_{600} = 3.0, cells were harvested *via* centrifugation at 8000*g* for 5 min. The resulting cell pellets were then washed with 25 mL of S30 buffer (10 mM Tris acetate pH 8.2, 14 mM magnesium acetate, and 60 mM potassium acetate) *via* vortexing in cycles of 15 s vortexing and 15 s on ice. After resuspension, cell pellets were centrifuged at 10,000*g* for 2 min, and the supernatant was poured off the cell pellet. The wash step was then repeated for a total of 3 washes. After the final wash step, cell pellets were massed, and 1 mL of S30 buffer was added per 1 g of cell mass. Cells were then resuspended *via* vortexing, again in cycles of 15 s vortexing and 15 s on ice. After resuspension, the cells were then lysed *via* homogenization using a single pass through an Avestin EmulsiFlex-B15 at 20,000−25,000 psig. Following homogenization, the lysed cell solution was separated into 1 mL aliquots and centrifuged at 12,000*g* for 10 min. The supernatant was then collected and again centrifuged at 12,000*g* for 10 min. After this final spin, the supernatant was pooled together, aliquoted, flash frozen, and stored at −80 °C until use.

For cell extracts derived from CLM24 cells, the above directions provided for BL21 Star™ (DE3) cell extracts were followed without inducing T7 RNA polymerase expression. Additionally, the supernatant from the first 12,000*g* centrifugation spin after cell lysis underwent a runoff reaction by wrapping the tubes in aluminum foil and incubating for 1 h at 37 °C and agitation at 250 RPM.

For cell extracts derived from SCM6 cells, the directions provided for extracts derived from CLM24 cells were followed.

For PglB overexpression in cell extracts derived from CLM24 Δ*lpxM* cells, the above directions provided for BL21 Star™ (DE3) cell extracts were performed with the following changes. Prior to cell growth, electrocompetent cells were transformed with pSF-CjPglB^{N311V}-LpxE-KanR and plated on LB agar plates containing 50 μg/mL of kanamycin. Prior to cell growth, the media were also supplemented with 50 μg/mL of kanamycin. At OD_{600} = 0.6−0.8, rather than inducing for T7 RNA polymerase expression with IPTG, expression of PglB was induced by adding arabinose to a final concentration of 0.1% w/v, and the culture was shifted to incubation at 30 °C with an agitation rate of 220 rpm. Additionally, the supernatant from the first 12,000*g* centrifugation spin after cell lysis underwent runoff by wrapping the tubes in aluminum foil and incubating for 1 h at 37 °C and agitation at 250 rpm.

For PglB overexpression in cell extracts derived from SCM6 cells, the above directions for extracts derived from CLM24 Δ*lpxM* cells were followed with the exception of growing in media without glucose (2xYTP) and inducing for expression of PglB at OD_{600} 0.6−0.8 with arabinose added at a final concentration of 0.02% w/v.

For cell extracts derived from 759.T7.opt cells, the above directions provided for BL21 Star™ (DE3) cell extracts were performed with the following changes. All cell cultures were incubated at 34 °C. After the wash steps, the cell pellet was resuspended in 0.8 mL of S30 buffer per gram of cell mass. Rather than homogenization for cell lysis, cells were lysed *via* sonication with a Q125 Sonicator (Qsonica) by submerging 1 mL aliquots in an ice/water slurry and using 45 s on and 59 s off cycles at 50% amplitude until ∼705 J was reached.

Cell-Free Protein Synthesis Reactions. All cell-free protein synthesis (CFPS) reactions using extracts derived from BL21 Star™ (DE3) or 759.T7.opt cells were set up using a modified PANOx-SP system.[71−74] Briefly, each reaction was assembled by mixing the following components: 8 mM magnesium glutamate; 10 mM ammonium glutamate; 130 mM potassium glutamate; 1.2 mM ATP; 0.85 mM GTP; 0.85 mM UTP; 0.85 mM CTP; 34 μg/mL folinic acid; 0.17 mg mL^{-1} tRNA; 0.4 mM nicotinamide adenine dinucleotide (NAD); 0.27 mM coenzyme A (CoA); 4 mM oxalic acid; 1 mM putrescine; 1.50 mM spermidine; 57 mM HEPES, pH 7.2; 2 mM of each of the 20 standard amino acids, 33 mM phosphoenolpyruvate (PEP), 13.33 ng/μL plasmid template, and 30% v/v cell extract. All of the reactions were incubated at 30 °C.

CFPS reactions using extracts derived from CLM24, SCM6, and CLM24 ΔlpxM cells were setup as described above with the addition of 0.1 mg mL^{-1} T7 RNA polymerase in 50% w/v glycerol and were run with 10 mM magnesium glutamate instead of 8 mM magnesium glutamate.

https://doi.org/10.1021/acschembio.4c00228
ACS Chem. Biol. 2024, 19, 1570−1582

Nanodisc-supplemented CFPS reactions expressing PglB were supplemented with 2 μL of nanodisc MSP1E3D1 POPC (Cube Biotech) per 15 μL of reaction mixture and were incubated overnight.

The sfGFP acceptor protein was expressed in the lysates described in Table 2 depending on the requirements of each experiment, and the CFPS reaction was incubated for 4 h. Elaboration enzymes LgtB and PdST6 were expressed in 759.T7.Opt to obtain as much enzyme as possible and were incubated for 4 h. LgtB is subject to proteolytic degradation, so it is important to limit CPFS incubation time and prevent overnight CFPS reactions.

***In Vitro* Glycosylation (IVG) Reactions.** *In vitro* glycosylation (IVG) reactions[28,75] were run in 50 mM HEPES pH 7.4 buffer. The total volume of all reactions was 40 μL. Various final concentrations of manganese chloride, activated sugar donors, acceptor protein produced in CFPS, PglB produced in nanodiscs or present in enriched extract, elaboration glycosyltransferases, Ficoll-400, and DDM were used for each figure. These conditions are summarized in Table 2. After all components were mixed, while the manganese chloride solution was added last because of its propensity to precipitate proteins, reactions were incubated at 30 °C overnight. For Figure 5 "with purification" sample, the GlcNAcylation reaction was first run overnight with the $MnCl_2$, UDP-GlcNAc, PglB N311V, and the sfGFP acceptor protein expressed in CFPS. The samples were then purified by adding 40 μL of the wash buffer (50 mM sodium phosphate, pH 7.4, 300 mM NaCl, 10 mM imidazole) to each sample and spinning samples at 16,100*g* at 4 °C for 10 min. The soluble fractions were added to 30 μL of Dynabead His-Tag Isolation and Pulldown magnetic beads pre-equilibrated in the wash buffer. Samples were incubated with rotation at 4 °C for 45 min. Samples were then washed three times in 100 μL of wash buffer and resuspended in 10 μL of elution buffer (50 mM sodium phosphate, pH 7.4, 300 mM NaCl, 500 mM imidazole). Samples were incubated with rotation at 4 °C for 30 min to complete the elution, and the supernatant was collected and buffer exchanged with Zeba spin columns (75 μL, 7 kDa MWCO) to 50 mM HEPES, pH 7.4, 150 mM NaCl following manufacturer's instructions, using 3 μL of stacker buffer.

Tandem Liquid Chromatography–Mass Spectrometry (LC-MS). After IVG reactions, samples were spun at 16,100*g* at 4 °C for 10 min. The samples were purified by adding the soluble fraction to 30 μL of IBA MagStrep "type 3" Strep-Tactin magnetic beads pre-equilibrated in wash buffer (IBA buffer W) and incubating at 4 °C with rotation for at least 30 min. The samples were washed three times with 100 μL of wash buffer before being placed in 40 μL of elution buffer (IBA buffer BXT) and incubated at 4 °C with rotation for at least 15 min. Purified samples were buffer exchanged to 50 mM HEPES pH 7.4, 150 mM NaCl using Zeba spin columns (0.5 mL, 7 kDa MWCO) following manufacturer's instructions and using 15 μL of stacker buffer. Trypsin (Promega) was added to a final concentration of 0.003 mg mL^{-1} to the samples and incubated for at least 1.5 h. C18 peptide cleanup spin columns (Agilent) were then used to clean up the samples following manufacturer's instructions. After elution, samples were completely evaporated in a vacuum evaporator and resuspended in 25 μL of nuclease-free water. Samples were spun at 21,000*g* at 4 °C for 10 min before being loaded into HPLC vials. Five μL of sample was injected on a

Table 2. An Overview of the IVG Reaction Conditions is Given in Each Figure

IVG component	Figure 2	Figure 3b–e	Figure 3f (optimized conditions)	Figure 4	Figure 5 (one step)	Figure 5 (two steps)
$MnCl_2$	10 mM	10 mM	8.75 mM	8.75 mM	8.75 mM	8.75 mM
UDP-GlcNAc	30 mM	30 mM	20 mM	15 mM	20 mM	50 mM (before purification)
UDP-Galactose	0 mM	0 mM	0 mM	0 mM	10 mM	50 mM (after purification)
CMP-Sialic Acid	0 mM	0 mM	0 mM	0 mM	10 mM	50 mM (after purification)
PglB	20% (v/v) of ND CFPS (BL21 Star (DE3)	20% (v/v) of enriched extract (CLM24)	20% (v/v) of enriched extract (CLM24)	25% (v/v) of enriched extract (CLM24/SCM6) (varies from 5% to 50% in Supplementary Figure 17)	20% (v/v) of enriched extract (CLM24)	40% (v/v) of enriched extract (CLM24)
LgtB	0	0	0	0	15% (v/v) of CFPS (759.T7.Opt)	25% (v/v) of CPFS (759.T7.Opt)
PdST6	0	0	0	0	25% (v/v) of CFPS (759.T7.Opt)	25% (v/v) of CFPS (759.T7.Opt)
sfGFP Acceptor CFPS	30% (v/v) of CFPS (BL21 Star (DE3)	30% (v/v) of CFPS (BL21 Star (DE3)	10% (v/v) of CFPS (CLM24 enriched extract)	10% (v/v) of CFPS (SCM6 extract – no enrichment)	2.5% (v/v) of CFPS (759.T7.Opt)	20% (v/v) of enriched extract (CLM24) or purified GlcNAcylated protein
Ficoll-400	1%	1%	0%	0%	0%	0%
DDM	0.1%	0%	0%	0%	0%	0%

https://doi.org/10.1021/acschembio.4c00228
ACS Chem. Biol. 2024, 19, 1570–1582

1290 Infinity II UHPLC System (Agilent Technologies Inc., Santa Clara, California, USA) onto a Poroshell 120 EC-C18 column (1.9 μm, 50 × 2.1 mm) (Agilent Technologies Inc., Santa Clara, California, USA) for C-18 chromatography, which was maintained at 40 °C with a constant flow rate at 0.400 ml/min, using a gradient of mobile phase A (water, 0.1% formic acid) and mobile phase B (100% acetonitrile, 0.1% formic acid). The gradient program was as follows: 0 − 1 min, 5%B; 1 − 8 min, 5 − 100%B; 8 − 10 min, hold 100%B; 10 − 10.10 min, 100 − 5%B; 10.10 − 15 min, hold 5%B. "MS-Only" positive ion mode acquisition was conducted on the samples on an Agilent 6545 quadrupole time-of-flight mass spectrometer equipped with a JetStream ionization source. The source conditions were as follows: gas temperature, 300 °C; drying gas flow, 12 L/min; nebulizer, 60 psi; sheath gas temperature, 400 °C; sheath gas flow, 11 L/min; VCap, 3500 V; fragmentor, 170 V; skimmer, 65 V; and Oct 1 RF, 750 V. The acquisition rate in MS-Only mode was 2 spectra/s, from m/z 100 to 1700 m/z range and utilizing m/z 121.05087300 and m/z 922.00979800 as reference masses. The liquid chromatography method for the MS/MS fragmentation was identical to that above. Both the + 4 and + 3 charge states of the aglycosylated and GlcNAcylated peptides were targeted (911.669, 1215.223, 962.439, and 1282.916) for fragmentation with a ramped collision energy with a slope that was 3.6 with an offset of −3.8. Other MS parameters remained identical with those described above.

Sample files were imported to Agilent MassHunter B10.0 Qualitative Analysis B10.0. The *N*-GlcNAcylation efficiency was calculated by taking the ratio of the area under the curve of the EIC for the + 4 charge state corresponding to the mass to charge ratio of the GlcNAcylated species to the total area under the curve of the EIC for both the aglycosylated and GlcNAcylated species. Similarly, the relative abundances of the trisaccharide species were calculated by taking the ratio of the area under the curve of the EIC for the designated species to the sum of the areas under the curve of all the species.

Definitive Screening Design Setup. Definitive screening design experiments were designed in JMP Pro 17 by using the definitive screening design tab. No blocks were used, and 4 extra runs were used for both experiments to improve power. The run order was randomized by the software. After data collection, data were analyzed using the fit definitive screening tab in the software.

Western Blotting. Samples were loaded on a 4−12% Bis-Tris gel and run with MES SDS running buffer for 45 min at 200 V. Samples were then transferred to Immobilon-P-poly(vinylidene difluoride) (PVDF) 0.45 μm membranes for 45 min at 80 mA per blot using a semidry transfer cell. Following transfer, the membranes were blocked for 30 min at RT in intercept blocking buffer. Following blocking, the membranes were then probed for 1 h at RT using an FITC-conjugated anti-FLAG tag antibody (Abcam Ab2492) at 1:7500 dilution in intercept blocking buffer supplemented with 0.2% Tween20. Following primary antibody incubation, the blots were then washed five times for 5 min with 1 × PBST at RT. After washing, a fluorescent goat, anti-rabbit GAR-680RD (LI-COR 926−68071) antibody was used as the secondary antibody at a dilution of 1:10,000 in intercept blocking buffer supplemented with 0.2% Tween20 and 0.001% SDS. Following a 1-h incubation at RT in the secondary antibody, the blots were again washed five times for 5 min with 1 × PBST followed by one wash for 5 min in 1 × PBS. Blots were imaged using an Odyssey Fc Imager (LI-COR) and images were analyzed by densitometry using Licor Image Studio.

■ ASSOCIATED CONTENT

Supporting Information

The Supporting Information is available free of charge at https://pubs.acs.org/doi/10.1021/acschembio.4c00228.

Detailed mass spectra to support glycosylation quantification shown in the main text; CID MS/MS fragmentation spectra to support GlcNAcylation observed in Figure 2 and the presence of the aglycosylated species in Figure 3; a summary of the conditions and results of the definitive screening design experiment to improve glycosylation efficiency; glycosylation efficiency of all the controls for the optimized conditions for both wild-type and PglB^{N311V}; characterization of the expression of PglB in enriched extracts by Western blot and corresponding volume adjustments to correct for glycosyltransferase when determining the necessity of WecA for the successful GlcNAcylation of the acceptor protein; a summary and results of the definitive screening design experiment for the elaboration of GlcNAc with lactose and sialic acid (PDF)

■ AUTHOR INFORMATION

Corresponding Author

Michael C. Jewett − *Department of Bioengineering, Stanford University, Stanford, California 94305, United States;* orcid.org/0000-0003-2948-6211; Phone: (+1) 847 467 5007; Email: mjewett@stanford.edu

Authors

Madison A. DeWinter − *Medical Scientist Training Program, Northwestern University Feinberg School of Medicine, Chicago, Illinois 60611, United States; Department of Chemical and Biological Engineering, Northwestern University, Evanston, Illinois 60208, United States; Chemistry of Life Processes Institute and Center for Synthetic Biology, Northwestern University, Evanston, Illinois 60208, United States;* orcid.org/0000-0001-8637-9995

Derek A. Wong − *Department of Chemical and Biological Engineering, Northwestern University, Evanston, Illinois 60208, United States; Chemistry of Life Processes Institute and Center for Synthetic Biology, Northwestern University, Evanston, Illinois 60208, United States;* orcid.org/0000-0002-1405-7310

Regina Fernandez − *Department of Chemical and Biological Engineering, Northwestern University, Evanston, Illinois 60208, United States; Chemistry of Life Processes Institute and Center for Synthetic Biology, Northwestern University, Evanston, Illinois 60208, United States*

Weston Kightlinger − *Cell-free Protein Synthesis and Microbial Process Development, National Resilience Inc.,, Oakland, California 94606, United States;* orcid.org/0000-0002-5264-4866

Ariel Helms Thames − *Medical Scientist Training Program, Northwestern University Feinberg School of Medicine, Chicago, Illinois 60611, United States; Department of Chemical and Biological Engineering, Northwestern University, Evanston, Illinois 60208, United States; Chemistry of Life Processes Institute and Center for Synthetic*

https://doi.org/10.1021/acschembio.4c00228
ACS Chem. Biol. 2024, 19, 1570−1582

Biology, Northwestern University, Evanston, Illinois 60208, United States; Division of Allergy and Immunology, Department of Medicine, Northwestern University Feinberg School of Medicine, Chicago, Illinois 60611, United States; orcid.org/0000-0001-5418-6048

Matthew P. DeLisa − *Robert Frederick Smith School of Chemical and Biomolecular Engineering and Cornell Institute of Biotechnology, Cornell University, Ithaca, New York 14853, United States*

Complete contact information is available at: https://pubs.acs.org/10.1021/acschembio.4c00228

Author Contributions

¶M.A.D. and D.A.W. contributed equally. M.A.D. designed research, performed experiments, performed mass spectrometry of all samples, analyzed data, and wrote the paper. D.A.W designed research, performed experiments, analyzed data, and wrote the paper. R.F. performed experiments and analyzed mass spectrometry data. W.K. designed research and edited the paper. A.H.T. designed research and edited the paper. M.P.D. designed research and edited the paper. M.C.J. designed and directed research, analyzed data, and wrote the paper.

Notes

The authors declare the following competing financial interest(s): M.C.J. and M.P.D. have a financial interest in Resilience and Gauntlet Bio. M.C.J. also has a financial interest in Synolo Therapeutics, and Stemloop, Inc.. M.C.J.s interests are reviewed and managed by Northwestern University and Stanford University in accordance with their conflict-of-interest policies. M.P.D.s interests are reviewed and managed by Cornell University. M.C.J., M.A.D., and D.A.W., have filed a provisional patent application based on this work. All other authors declare no conflicts of interest.

■ ACKNOWLEDGMENTS

This work was supported by DTRA (HDTRA1-21-1-0038) and DARPA (W911NF-23-2-0039). D.A.W. acknowledges support from the National Science Foundation Graduate Research Fellowship under grant no. DGE-1842165. This work made use of the IMSERC MS facility at Northwestern University, which has received support from the Soft and Hybrid Nanotechnology Experimental (SHyNE) Resource (NSF ECCS-2025633), the State of Illinois, and the International Institute for Nanotechnology (IIN). We thank F. Tobias and B. Owen for guidance and training on mass spectrometry.

■ REFERENCES

(1) Tsuda, E.; Kawanishi, G.; Ueda, M.; Masuda, S.; Sasaki, R. The role of carbohydrate in recombinant human erythropoietin. *Eur. J. Biochem.* **1990**, *188*, 405−411.

(2) Ueda, T.; Tomita, K.; Notsu, Y.; Ito, T.; Fumoto, M.; Takakura, T.; Nagatome, H.; Takimoto, A.; Mihara, S.-I.; Togame, H.; Kawamoto, K; Iwasaki, T.; Asakura, K.; Oshima, T.; Hanasaki, K.; Nishimura, S.-I.; Kondo, H. Chemoenzymatic Synthesis of Glycosylated Glucagon-like Peptide 1: Effect of Glycosylation on Proteolytic Resistance and in Vivo Blood Glucose-Lowering Activity. *J. Am. Chem. Soc.* **2009**, *131*, 6237−6245.

(3) Zheng, K.; Bantog, C.; Bayer, R. The impact of glycosylation on monoclonal antibody conformation and stability. *MAbs* **2011**, *3*, 568−576.

(4) Qin, K.; Shi, W.; Zhao, L.; Li, M.; Tang, Y.; Faridoon; Jiang, B.; Tang, F.; Huang, W. Thermostability detection and optimization of glycoengineered antibodies and antibody-drug conjugates based on differential scanning flouremitry analysis. *Bioorg. Chem.* **2020**, *94*, 103391.

(5) Abès, R.; Teillaud, J.-L. Impact of Glycosylation on Effector Functions of Therapeutic IgG. *Pharmaceuticals* **2010**, *3*, 146−157.

(6) Huang, W.; Giddens, J.; Fan, S. Q.; Toonstra, C.; Wang, L. X. Chemoenzymatic glycoengineering of intact IgG antibodies for gain of functions. *J. Am. Chem. Soc.* **2012**, *134*, 12308−12318.

(7) Shinkawa, T.; Nakamura, K.; Yamane, N.; Shoji-Hosaka, E.; Kanda, Y.; Sakurada, M.; Uchida, K.; Anazawa, H.; Satoh, M.; Yamasaki, M.; Hanai, N.; Shitara, K. The Absence of Fucose but Not the Presence of Galactose or Bisecting N-Acetylglucosamine of Human IgG1 Complex-type Oligosaccharides Shows the Critical Role of Enhancing Antibody-dependent Cellular Cytotoxicity*. *J. Biol. Chem.* **2003**, *278*, 3466−3473.

(8) Chung, C. H.; Mirakhur, B.; Chan, E.; Le, Q.-T.; Berlin, J.; Morse, M.; Murphy, B. A.; Satinover, S. M.; Hosen, J.; Mauro, D.; Slebos, R. J.; Zhou, Q.; Gold, D.; Hatley, T.; Hicklin, D. J.; Platts-Mills, T. A. E. Cetuximab-Induced Anaphylaxis and IgE Specific for Galactose-α-1,3-Galactose. *N. Engl. J. Med.* **2008**, *358*, 1109−1117.

(9) Esmail, S.; Manolson, M. F. Advances in understanding N-glycosylation structure, function, and regulation in health and disease. *Eur. J. Cell Biol.* **2021**, *100*, 151186.

(10) Chia, S.; Tay, S. J.; Song, Z.; Yang, Y.; Walsh, I.; Pang, K. T. Enhancing pharmacokinetic and pharmacodynamic properties of recombinant therapeutic proteins by manipulation of sialic acid content. *Biomed. Pharmacother.* **2023**, *163*, 114757.

(11) Anthony, R. M.; Ravetch, J. V. A Novel Role for the IgG Fc Glycan: The Anti-inflammatory Activity of Sialylated IgG Fcs. *J. Clin. Immunol.* **2010**, *30*, 9−14.

(12) Pagan, J. D.; Kitaoka, M.; Anthony, R. M. Engineered Sialylation of Pathogenic Antibodies In Vivo Attenuates Autoimmune Disease. *Cell* **2018**, *172*, 564−577.e13.

(13) Anthony, R. M.; Nimmerjahn, F. The role of differential IgG glycosylation in the interaction of antibodies with FcγRs in vivo. *Curr. Opin. Organ. Transplant.* **2011**, *16*, 7−14.

(14) Yamane-Ohnuki, N.; Satoh, M. Production of therapeutic antibodies with controlled fucosylation. *MAbs* **2009**, *1*, 230−236.

(15) Kightlinger, W.; Warfel, K. F.; DeLisa, M. P.; Jewett, M. C. Synthetic Glycobiology: Parts, Systems, and Applications. *ACS Synth. Biol.* **2020**, *9*, 1534−1562.

(16) Čaval, T.; Tian, W.; Yang, Z.; Clausen, H.; Heck, A. J. R. Direct quality control of glycoengineered erythropoietin variants. *Nat. Commun.* **2018**, *9*, 3342.

(17) Sasaki, H.; Ochi, N.; Dell, A.; Fukuda, M. Site-specific glycosylation of human recombinant erythropoietin: analysis of glycopeptides or peptides at each glycosylation site by fast atom bombardment-mass spectrometry. *Biochemistry* **1988**, *27*, 8618−8626.

(18) Narimatsu, Y.; Büll, C.; Chen, Y. H.; Wandall, H. H.; Yang, Z.; Clausen, H. Genetic glycoengineering in mammalian cells. *J. Biol. Chem.* **2021**, *296*, 100448.

(19) Meuris, L.; Santens, F.; Elson, G.; Festjens, N.; Boone, M.; Dos Santos, A.; Devos, S.; Rousseau, F.; Plets, E.; Houthuys, E.; et al. GlycoDelete engineering of mammalian cells simplifies N-glycosylation of recombinant proteins. *Nat. Biotechnol.* **2014**, *32*, 485−489.

(20) Thooft, K.; Van Breedam, W.; Santens, F.; Wyseure, E.; Vanmarcke, S.; Devos, S.; Callewaert, N.; Madder, A. GlyConnect-Ugi: site-selective, multi-component glycoprotein conjugations through GlycoDelete expressed glycans. *Org. Biomol. Chem.* **2022**, *20*, 464−471.

(21) Xu, Y.; Wu, Z.; Zhang, P.; Zhu, H.; Zhu, H.; Song, Q.; Wang, L.; Wang, F.; Wang, P. G.; Cheng, J. A novel enzymatic method for synthesis of glycopeptides carrying natural eukaryotic N-glycans. *Chem. Commun.* **2017**, *53*, 9075−9077.

(22) Makrydaki, E.; Donini, R.; Krueger, A.; Royle, K.; Moya Ramirez, I.; Kuntz, D. A.; Rose, D. R.; Haslam, S. M.; Polizzi, K. M.; Kontoravdi, C. Immobilized enzyme cascade for targeted glycosylation. *Nat. Chem. Biol.* **2024**, *20*, 732.

(23) Ahangama Liyanage, L.; Harris, M. S.; Cook, G. A. In Vitro Glycosylation of Membrane Proteins Using N-Glycosyltransferase. *ACS Omega* **2021**, *6*, 12133−12142.
(24) Adams, T. M.; Zhao, P.; Chapla, D.; Moremen, K. W.; Wells, L. Sequential in vitro enzymatic N-glycoprotein modification reveals site-specific rates of glycoenzyme processing. *J. Biol. Chem.* **2022**, *298*, 102474.
(25) Jaroentomeechai, T.; Stark, J. C.; Natarajan, A.; Glasscock, C. J.; Yates, L. E.; Hsu, K. J.; Mrksich, M.; Jewett, M. C.; DeLisa, M. P. Single-pot glycoprotein biosynthesis using a cell-free transcription-translation system enriched with glycosylation machinery. *Nat. Commun.* **2018**, *9*, 2686.
(26) Aquino, A.; Manzer, Z. A.; Daniel, S.; DeLisa, M. P. Glycosylation-on-a-chip: A Flow-Based Microfluidic System for Cell-Free Glycoprotein Biosynthesis. *Front. Mol. Biosci.* **2021**, *8*, 782905.
(27) Natarajan, A.; Jaroentomeechai, T.; Cabrera-Sánchez, M.; Mohammed, J. C.; Cox, E. C.; Young, O.; Shajahan, A.; Vilkhovoy, M.; Vadhin, S.; Varner, J. D.; et al. Engineering orthogonal human O-linked glycoprotein biosynthesis in bacteria. *Nat. Chem. Biol.* **2020**, *16*, 1062−1070.
(28) Guarino, C.; DeLisa, M. P. A prokaryote-based cell-free translation system that efficiently synthesizes glycoproteins. *Glycobiology* **2012**, *22*, 596−601.
(29) Hershewe, J.; Kightlinger, W.; Jewett, M. C. Cell-free systems for accelerating glycoprotein expression and biomanufacturing. *J. Ind. Microbiol. Biotechnol.* **2020**, *47*, 977−991.
(30) Stark, J. C.; Jaroentomeechai, T.; Warfel, K. F.; Hershewe, J. M.; DeLisa, M. P.; Jewett, M. C. Rapid biosynthesis of glycoprotein therapeutics and vaccines from freeze-dried bacterial cell lysates. *Nat. Protoc.* **2023**, *18*, 2374−2398.
(31) Jaroentomeechai, T.; Kwon, Y. H.; Liu, Y.; Young, O.; Bhawal, R.; Wilson, J. D.; Li, M.; Chapla, D. G.; Moremen, K. W.; Jewett, M. C.; et al. A universal glycoenzyme biosynthesis pipeline that enables efficient cell-free remodeling of glycans. *Nat. Commun.* **2022**, *13*, 6325.
(32) Warfel, K. F.; Laigre, E.; Sobol, S. E.; Gillon, E.; Varrot, A.; Renaudet, O.; Dejeu, J.; Jewett, M. C.; Imberty, A. Cell-free expression and characterization of multivalent rhamnose-binding lectins using bio-layer interferometry. *Glycobiology* **2023**, *33*, 358−363.
(33) Hershewe, J. M.; Warfel, K. F.; Iyer, S. M.; Peruzzi, J. A.; Sullivan, C. J.; Roth, E. W.; DeLisa, M. P.; Kamat, N. P.; Jewett, M. C. Improving cell-free glycoprotein synthesis by characterizing and enriching native membrane vesicles. *Nat. Commun.* **2021**, *12*, 2363.
(34) Liu, F.; Vijayakrishnan, B.; Faridmoayer, A.; Taylor, T. A.; Parsons, T. B.; Bernardes, G. J. L.; Kowarik, M.; Davis, B. G. Rationally Designed Short Polyisoprenol-Linked PglB Substrates for Engineered Polypeptide and Protein N-Glycosylation. *J. Am. Chem. Soc.* **2014**, *136*, 566−569.
(35) Napiórkowska, M.; Boilevin, J.; Sovdat, T.; Darbre, T.; Reymond, J.-L.; Aebi, M.; Locher, K. P. Molecular basis of lipid-linked oligosaccharide recognition and processing by bacterial oligosaccharyltransferase. *Nat. Struct. Mol. Biol.* **2017**, *24*, 1100−1106.
(36) Schwarz, F.; Huang, W.; Li, C.; Schulz, B. L.; Lizak, C.; Palumbo, A.; Numao, S.; Neri, D.; Aebi, M.; Wang, L.-X. A combined method for producing homogeneous glycoproteins with eukaryotic N-glycosylation. *Nat. Chem. Biol.* **2010**, *6*, 264−266.
(37) Li, H.; Zhang, J.; An, C.; Dong, S. Probing N-Glycan Functions in Human Interleukin-17A Based on Chemically Synthesized Homogeneous Glycoforms. *J. Am. Chem. Soc.* **2021**, *143*, 2846−2856.
(38) Cohen-Anisfeld, S. T.; Lansbury, P. T. A practical, convergent method for glycopeptide synthesis. *J. Am. Chem. Soc.* **1993**, *115*, 10531−10537.
(39) Wang, P.; Li, X.; Zhu, J.; Chen, J.; Yuan, Y.; Wu, X.; Danishefsky, S. J. Encouraging Progress in the ω-Aspartylation of Complex Oligosaccharides as a General Route to β-N-Linked Glycopolypeptides. *J. Am. Chem. Soc.* **2011**, *133*, 1597−1602.
(40) Joseph, R.; Dyer, F. B.; Garner, P. Rapid Formation of N-Glycopeptides via Cu(II)-Promoted Glycosylative Ligation. *Org. Lett.* **2013**, *15*, 732−735.
(41) Silverman, A. D.; Karim, A. S.; Jewett, M. C. Cell-free gene expression: an expanded repertoire of applications. *Nat. Rev. Genet.* **2020**, *21*, 151−170.
(42) Stark, J. C.; Jaroentomeechai, T.; Moeller, T. D.; Hershewe, J. M.; Warfel, K. F.; Moricz, B. S.; Martini, A. M.; Dubner, R. S.; Hsu, K. J.; Stevenson, T. C.; et al. On-demand biomanufacturing of protective conjugate vaccines. *Sci. Adv.* **2021**, *7*, No. eabe9444.
(43) Warfel, K. F.; Williams, A.; Wong, D. A.; Sobol, S. E.; Desai, P.; Li, J.; Chang, Y.-F.; DeLisa, M. P.; Karim, A. S.; Jewett, M. C. A Low-Cost, Thermostable, Cell-Free Protein Synthesis Platform for On-Demand Production of Conjugate Vaccines. *ACS Synth. Biol.* **2023**, *12*, 95−107.
(44) Williams, A. J.; Warfel, K. F.; Desai, P.; Li, J.; Lee, J.; Wong, D. A.; Nguyen, P. M.; Qin, Y.; Sobol, S. E.; Jewett, M. C.; Chang, Y.; DeLisa, M. P. A low-cost recombinant glycoconjugate vaccine confers immunogenicity and protection against enterotoxigenic Escherichia coli infections in mice. *Front. mol. biosci.* **2023**, *10*, 1085887.
(45) Thames, A. H.; Moons, S. J.; Wong, D. A.; Boltje, T. J.; Bochner, B. S.; Jewett, M. C. GlycoCAP: A Cell-Free, Bacterial Glycosylation Platform for Building Clickable Azido-Sialoglycoproteins. *ACS Synth. Biol.* **2023**, *12*, 1264−1274.
(46) Kightlinger, W.; Lin, L.; Rosztoczy, M.; Li, W.; DeLisa, M. P.; Mrksich, M.; Jewett, M. C. Design of glycosylation sites by rapid synthesis and analysis of glycosyltransferases. *Nat. Chem. Biol.* **2018**, *14*, 627−635.
(47) Kightlinger, W.; Duncker, K. E.; Ramesh, A.; Thames, A. H.; Natarajan, A.; Stark, J. C.; Yang, A.; Lin, L.; Mrksich, M.; DeLisa, M. P.; et al. A cell-free biosynthesis platform for modular construction of protein glycosylation pathways. *Nat. Commun.* **2019**, *10*, 5404.
(48) Ihssen, J.; Haas, J.; Kowarik, M.; Wiesli, L.; Wacker, M.; Schwede, T.; Thöny-Meyer, L. Increased efficiency of Campylobacter jejuni N-oligosaccharyltransferase PglB by structure-guided engineering. *Open Biology* **2015**, *5*, 140227.
(49) Feldman, M. F.; Wacker, M.; Hernandez, M.; Hitchen, P. G.; Marolda, C. L.; Kowarik, M.; Morris, H. R.; Dell, A.; Valvano, M. A.; Aebi, M. Engineering N-linked protein glycosylation with diverse O antigen lipopolysaccharide structures in Escherichia coli. *Proc. Natl. Acad. Sci. U. S. A.* **2005**, *102*, 3016−3021.
(50) Wacker, M.; Wang, L.; Kowarik, M.; Dowd, M.; Lipowsky, G.; Faridmoayer, A.; Shields, K.; Park, S.; Alaimo, C.; Kelley, K. A.; et al. Prevention of Staphylococcus aureus infections by glycoprotein vaccines synthesized in Escherichia coli. *J. Infect. Dis.* **2014**, *209*, 1551−1561.
(51) Garcia-Quintanilla, F.; Iwashkiw, J. A.; Price, N. L.; Stratilo, C.; Feldman, M. F. Production of a recombinant vaccine candidate against Burkholderia pseudomallei exploiting the bacterial N-glycosylation machinery. *Front. Microbiol.* **2014**, *5*, 381.
(52) Ravenscroft, N.; Braun, M.; Schneider, J.; Dreyer, A. M.; Wetter, M.; Haeuptle, M. A.; Kemmler, S.; Steffen, M.; Sirena, D.; Herwig, S.; et al. Characterization and immunogenicity of a Shigella flexneri 2a O-antigen bioconjugate vaccine candidate. *Glycobiology* **2019**, *29*, 669−680.
(53) Ravenscroft, N.; Haeuptle, M. A.; Kowarik, M.; Fernandez, F. S.; Carranza, P.; Brunner, A.; Steffen, M.; Wetter, M.; Keller, S.; Ruch, C.; Wacker, M. Purification and characterization of a Shigella conjugate vaccine, produced by glycoengineering *Escherichia coli*. *Glycobiology* **2016**, *26*, 51−62.
(54) Lizak, C.; Gerber, S.; Michaud, G.; Schubert, M.; Fan, Y.-Y.; Bucher, M.; Darbre, T.; Aebi, M.; Reymond, J.-L.; Locher, K. P. Unexpected reactivity and mechanism of carboxamide activation in bacterial N-linked protein glycosylation. *Nat. Commun.* **2013**, *4*, 2627.
(55) Ielmini, M. V.; Feldman, M. F. Desulfovibrio desulfuricans PglB homolog possesses oligosaccharyltransferase activity with relaxed glycan specificity and distinct protein acceptor sequence requirements†. *Glycobiology* **2011**, *21*, 734−742.

https://doi.org/10.1021/acschembio.4c00228
ACS Chem. Biol. 2024, 19, 1570−1582

(56) Ihssen, J.; Kowarik, M.; Wiesli, L.; Reiss, R.; Wacker, M.; Thöny-Meyer, L. Structural insights from random mutagenesis of Campylobacter jejunioligosaccharyltransferase PglB. *BMC Biotechnology* **2012**, *12*, 67.
(57) Kowarik, M.; Young, N. M.; Numao, S.; Schulz, B. L.; Hug, I.; Callewaert, N.; Mills, D. C.; Watson, D. C.; Hernandez, M.; Kelly, J. F.; et al. Definition of the bacterial N-glycosylation site consensus sequence. *Embo J.* **2006**, *25*, 1957−1966.
(58) Chen, M. M.; Glover, K. J.; Imperiali, B. From Peptide to Protein: Comparative Analysis of the Substrate Specificity of N-Linked Glycosylation in C. jejuni. *Biochemistry* **2007**, *46*, 5579−5585.
(59) Ma, J.; Hart, G. W. Analysis of Protein O-GlcNAcylation by Mass Spectrometry. *Curr. Protoc. Protein Sci.* **2017**, *87*, 24.10.21−24.10.16.
(60) Ma, J.; Hart, G. W. O-GlcNAc profiling: from proteins to proteomes. *Clin. Proteomics* **2014**, *11*, 8.
(61) Jones, B.; Nachtsheim, C. J. A Class of Three-Level Designs for Definitive Screening in the Presence of Second-Order Effects. *Journal Of Quality Technology* **2011**, *43*, 1−15.
(62) Gerber, S.; Lizak, C.; Michaud, G.; Bucher, M.; Darbre, T.; Aebi, M.; Reymond, J. L.; Locher, K. P. Mechanism of bacterial oligosaccharyltransferase: in vitro quantification of sequon binding and catalysis. *J. Biol. Chem.* **2013**, *288*, 8849−8861.
(63) Napiórkowska, M.; Boilevin, J.; Darbre, T.; Reymond, J. L.; Locher, K. P. Structure of bacterial oligosaccharyltransferase PglB bound to a reactive LLO and an inhibitory peptide. *Sci. Re.p* **2018**, *8*, 16297.
(64) Wacker, M.; Feldman, M. F.; Callewaert, N.; Kowarik, M.; Clarke, B. R.; Pohl, N. L.; Hernandez, M.; Vines, E. D.; Valvano, M. A.; Whitfield, C.; et al. Substrate specificity of bacterial oligosaccharyltransferase suggests a common transfer mechanism for the bacterial and eukaryotic systems. *Proc. Natl. Acad. Sci.* **2006**, *103*, 7088−7093.
(65) Al-Dabbagh, B.; Mengin-Lecreulx, D.; Bouhss, A. Purification and Characterization of the Bacterial UDP-GlcNAc: Undecaprenyl-Phosphate GlcNAc-1-Phosphate Transferase WecA. *J. Bacteriol.* **2008**, *190*, 7141−7146.
(66) Ueda, T.; Ito, T.; Tomita, K.; Togame, H.; Fumoto, M.; Asakura, K.; Oshima, T.; Nishimura, S.-I.; Hanasaki, K. Identification of glycosylated exendin-4 analogue with prolonged blood glucose-lowering activity through glycosylation scanning substitution. *Bioorg. Med. Chem. Lett.* **2010**, *20*, 4631−4634.
(67) Tytgat, H. L. P.; Lin, C.-W.; Levasseur, M. D.; Tomek, M. B.; Rutschmann, C.; Mock, J.; Liebscher, N.; Terasaka, N.; Azuma, Y.; Wetter, M.; et al. Cytoplasmic glycoengineering enables biosynthesis of nanoscale glycoprotein assemblies. *Nat. Commun.* **2019**, *10*, 5403.
(68) Giddens, J. P.; Lomino, J. V.; Amin, M. N.; Wang, L. X. Endo-F3 Glycosynthase Mutants Enable Chemoenzymatic Synthesis of Core-fucosylated Triantennary Complex Type Glycopeptides and Glycoproteins. *J. Biol. Chem.* **2016**, *291*, 9356−9370.
(69) Fairbanks, A. J. The ENGases: versatile biocatalysts for the production of homogeneous N-linked glycopeptides and glycoproteins. *Chem. Soc. Rev.* **2017**, *46*, 5128−5146.
(70) Kwon, Y. C.; Jewett, M. C. High-throughput preparation methods of crude extract for robust cell-free protein synthesis. *Sci. Rep.* **2015**, *5*, 8663.
(71) Des Soye, B. J.; Gerbasi, V. R.; Thomas, P. M.; Kelleher, N. L.; Jewett, M. C. A Highly Productive, One-Pot Cell-Free Protein Synthesis Platform Based on Genomically Recoded Escherichia coli. *Cell Chem. Biol.* **2019**, *26*, 1743−1754.e1749.
(72) Martin, R. W.; Des Soye, B. J.; Kwon, Y.-C.; Kay, J.; Davis, R. G.; Thomas, P. M.; Majewska, N. I.; Chen, C. X.; Marcum, R. D.; Weiss, M. G.; Stoddart, A. E.; et al. Cell-free protein synthesis from genomically recoded bacteria enables multisite incorporation of noncanonical amino acids. *Nat. Commun.* **2018**, *9*, 1203−1203.10.1038/s41467−018−03469−5.
(73) Jewett, M. C.; Calhoun, K. A.; Voloshin, A.; Wuu, J. J.; Swartz, J. R. An integrated cell-free metabolic platform for protein production and synthetic biology. *Mol. Syst. Biol.* **2008**, *4*, 220.
(74) Jewett, M. C.; Swartz, J. R. Mimicking the Escherichia coli cytoplasmic environment activates long-lived and efficient cell-free protein synthesis. *Biotechnol. Bioeng.* **2004**, *86*, 19−26.
(75) Schoborg, J. A.; Hershewe, J. M.; Stark, J. C.; Kightlinger, W.; Kath, J. E.; Jaroentomeechai, T.; Natarajan, A.; DeLisa, M. P.; Jewett, M. C. A cell-free platform for rapid synthesis and testing of active oligosaccharyltransferases. *Biotechnol. Bioeng.* **2018**, *115*, 739−750.

https://doi.org/10.1021/acschembio.4c00228
ACS Chem. Biol. 2024, 19, 1570−1582